ANALYSIS OF THE ARRAY APPLICATOR COMPOSED OF COAXIAL-SLOT ANTENNAS FOR INTERSTITIAL MICROWAVE HYPERTHERMIA

Lira HAMADA, Koichi ITO
Department of Electrical and Electronics Engineering
Faculty of Engineering, Chiba University
1-33 Yayoi-cho, Inage-ku, Chiba-shi, 263 Japan

1.INTRODUCTION. Hyperthermia is a cancer treatment to heat tumors up to therapeutic temperatures (42-45°C) without overheating the surrounding normal tissue (1). The multiple coaxial-slot antenna is an applicator for interstitial microwave hyperthermia(2). The antenna is commonly used as an array applicator for large-volume tumors. In this paper the characteristics of the array applicator will be investigated theoretically by using the basic antenna structure with single-slot. Two array structures (a square array or a hexagonal array) and two operating frequencies (430 MHz or 915 MHz) are chosen to discuss their effect on both the current distribution and the SAR (specific absorption rate) distribution.

2. STRUCTURE OF THE ANTENNA. Fig. 1 shows the basic structure of a single coaxial-slot antenna, the element of the array applicator. It is made from a coaxial semi-rigid cable of 0.86 mm in outer diameter. A ring slot is cut on the outer conductor and the tip of the cable is short-circuited. A thin plastic catheter covers each array element for medical safety.

3. METHODS. The analysis model is depicted in Fig.2. For simplicity, the cable in the air is modeled with finite length. The human body is considered as homogeneous muscular tissue. The muscle medium and the air are referred to as medium 1 and medium 2. The relative complex permittivities of the muscle medium are 53-j59 at 430 MHz or 51-j31 at 915 MHz, and that of the catheter is 2.1. The catheter is replaced with the equivalent polarization current. The electric field source at the ring slot is replaced by a narrow strip of magnetic current, which is generated by feeding the voltage at the slot. The full-wave Green's function used is expressed by a series of exponential functions (2). The electric current distribution in the conductor of the antenna is calculated by using the moment method (3). The current distribution is approximated by a series of expansion functions F_n such that

$$F_n^{\mp}(z') = \frac{\sinh(jk_q|z'-z'_{n\mp1}|)}{\sinh(jk_q|z'_n-z'_{n\mp1}|)} \qquad (1)$$

$(F_n^- \text{ for } z'_{n-1} \le z' \le z'_n \text{ and } F_n^+ \text{ for } z'_n \le z' \le z'_{n+1})$

$$I(z') = \sum_{n=1}^{N} I_n F_n, \quad F_n = F_n^-(z') + F_n^+(z') \qquad (2)$$

where I_n is the unknown coefficient and $k_q = \omega\sqrt{\mu_o \varepsilon_o \varepsilon_{rq}}$ is the propagation constant in medium q (q=1,2). An equivalent polarization current J_c in the catheter is given by Ref.(4).

$$J_c(\rho, z') = j\omega\varepsilon_o(\varepsilon_{rc} - \varepsilon_{rq}) E_\rho = \frac{-(\varepsilon_{rc} - \varepsilon_{rq})}{2\pi\varepsilon_{rc}\rho}\left(\frac{dI(z')}{dz'}\right) \qquad (3)$$

According to the electric field boundary condition on the conductor of the antenna, the matrix form of the simultaneous linear equation is written as Eq.(4).

$$[Z_{mn}][I_n]=[V_m] \tag{4}$$

The current distribution will be derived from solving the matrix equations in Eq.(4).

Heating ability of the antenna is evaluated by the SAR distribution, which is defined as Eq.(5).

$$SAR=\frac{\sigma}{2\xi}|E|^2 \tag{5}$$

where σ is the conductivity, ξ is the density of medium and E is the electric field around the antenna. In the calculation, σ=1.41[S/m] at 430 MHz or 1.58 [S/m] at 915 MHz, and ξ=1000[kg/m^3] are used. Electric field distribution around the array is derived from the electric current distribution.

4. STRUCTURE OF THE ARRAY APPLICATOR. Fig.3 shows the structures of the square array and the hexagonal array. In this paper the array spacing As and the antenna insertion depth Dt are set at 15 [mm] or 70 [mm], respectively. The observation planes for the SAR distribution are shown in the Figure. All array elements are driven in the same feeding voltage and in phase.

5. CALCULATED RESULT. Figures 4 and 5 show the current distributions along an array element for various operating frequencies and for various array structures, respectively. The current distributions are changed in varying operating frequencies and array structures. Figures 6, 7 and 8 show calculated SAR distributions. Higher SAR is obtained at 915 MHz than at 430 MHz (See Figs, 6 and 7), and larger heating area is derived in t-plane of the hexagonal array than that of the square array (See Figs. 6 and 8).

6. CONCLUSION. We have discussed the effect of the structure of the array applicator and the operating frequency on heating characteristics of the array applicator; both on the current distribution and the SAR distribution. For theoretical study, a simplified analysis model has been proposed. These results are applicable to various clinical cases and are helpful for designing such type interstitial antennas.

REFERENCES. (1) J.W. Hand and J.R. James (Eds.) :" *Physical techniques in clinical hyperthermia*", Research Studies Press, UK, 1986.

(2) M. S. Wu, et.al. :"Analysis of current and electric field distributions of coaxial-slot antenna for interstitial microwave hyperthermia", Journal of Electromagnetic Waves and Application, Vol. 9, No. 5/6, pp. 831-849, 1995.

(3) W.L. Stutzman and G.A. Thiele :" *Antenna theory and design*", John Wiley & Sons, pp.306-339. 1981.

(4) J.H. Richmod and E.H. Newman :"Dielectric coated wire antennas", Radio Science. Vol.11, No.1, pp.13-20, 1976.

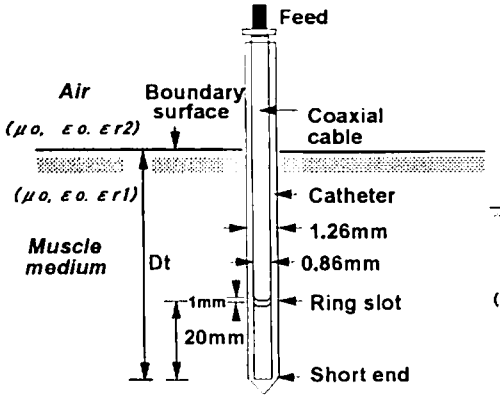

Fig.1 A single coaxial-slot antenna.

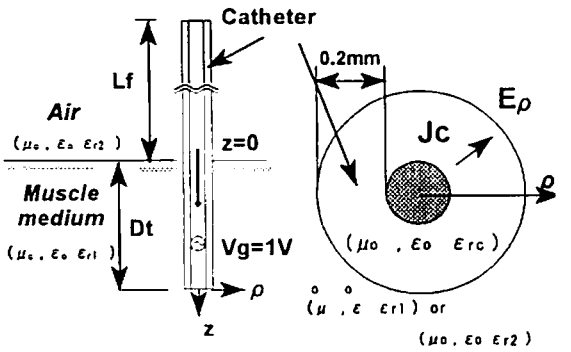

Fig.2 Analysis model.

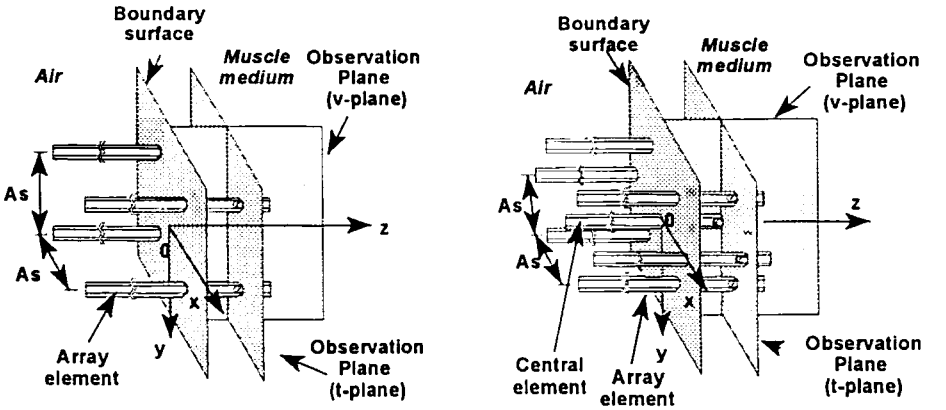

(a) The square array. (b) The hexagonal array.

Fig.3 Array structures and observation planes.

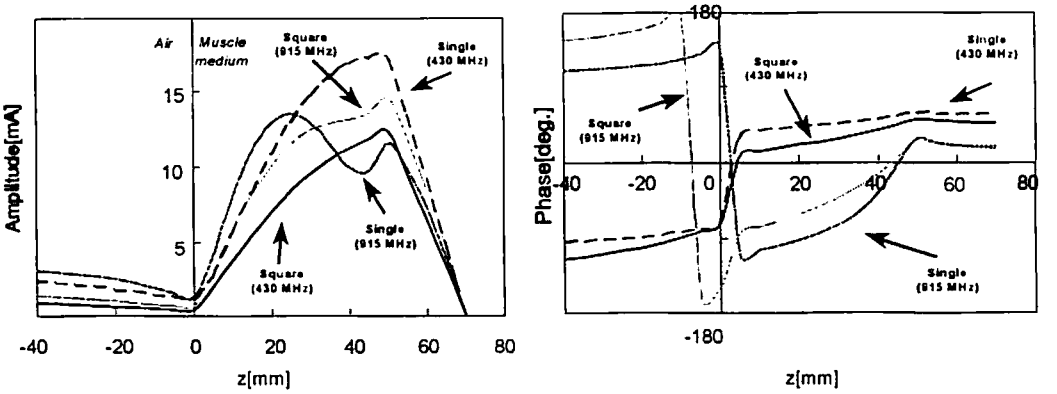

Amplitude Phase

Fig.4 Dependence of the current distribution on the operating frequency.

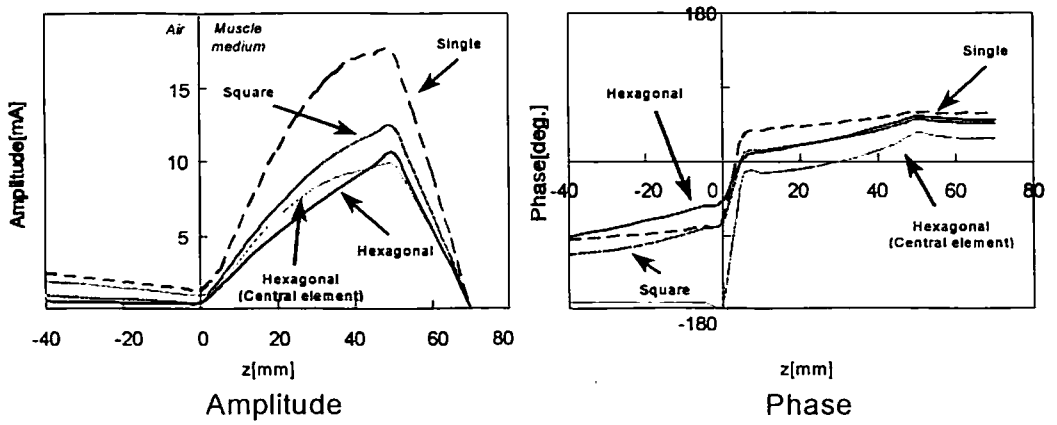

Amplitude Phase

Fig.5 Dependence of the current distribution on the array structure (430 MHz).

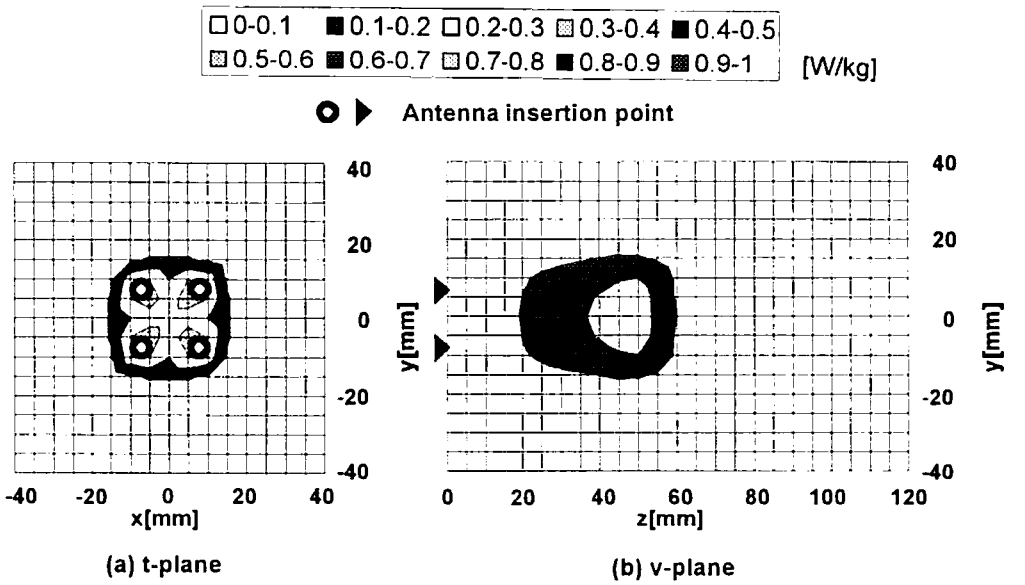

(a) t-plane (b) v-plane

Fig. 6 SAR distribution of the square array at 430 MHz.

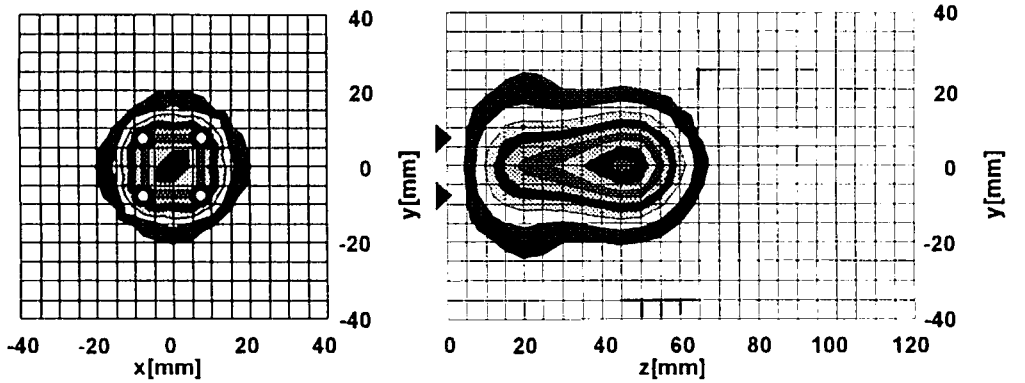

(a) t-plane (b) v-plane

Fig. 7 SAR distribution of the square array at 915 MHz.

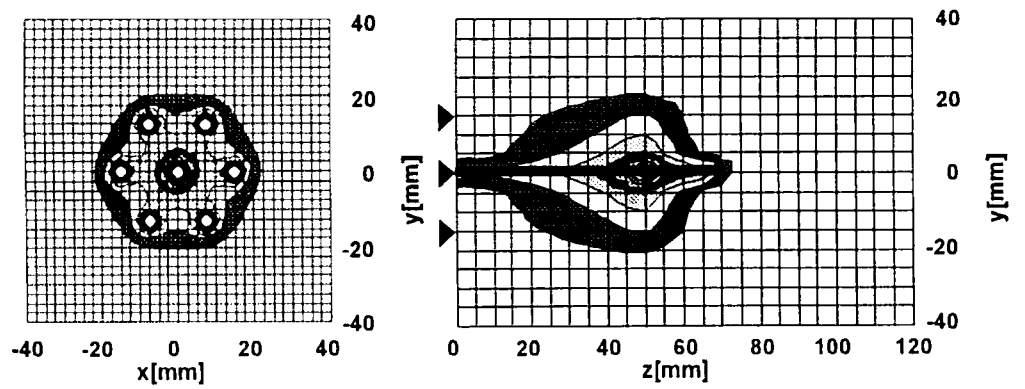

(a) t-plane (b) v-plane

Fig. 8 SAR distribution of the hexagonal array at 430 MHz.